

DEVELOPMENT OF A SMALL-SCALE SUPERSONIC FLIGHT EXPERIMENT VEHICLE AS A FLYING TEST BED

**Kazuhide MIZOBATA, Ryojiro MINATO, Kazuyuki HIGASHINO
and Nobuhiro TANATSUGU**

**Aerospace Plane Research Center, Muroran Institute of Technology, Japan
mizobata@mmm.muroran-it.ac.jp**

Keywords: *Supersonic, Flying Test Bed, Flight Test, Aerodynamics, Jet Propulsion*

Abstract

With the aims of creating and validating innovative fundamental technologies for high-speed atmospheric flights, a small scale supersonic experiment vehicle is designed as a flying test bed. Several aerodynamic configurations are proposed and analyzed by wind tunnel tests. A twin-engine configuration with a cranked-arrow main wing is selected as the baseline. Its flight capability is predicted by point mass analysis on the basis of aerodynamic characterization and propulsion performance estimation. In addition, a prototype vehicle with an almost equivalent configuration and dimension is designed and fabricated for verification of the subsonic flight characteristics of the experiment vehicle. Its first flight test is carried out and good flight capability is demonstrated. Furthermore a revised aerodynamic configuration with an air-turbo ramjet gas-generator cycle (ATR-GG) engine is being designed for improvement in flight capability at higher Mach numbers. Development of the engine, airframe structure, and autonomous guidance/control system is underway. This prospective flight experiment vehicle will be applied to flight verification of innovative fundamental technologies for high-speed atmospheric flights such as turbo-ramjet propulsion with endothermic or biomass fuels, MEMS and morphing techniques for aerodynamic control, aero-servo-elastic technologies, etc.

Nomenclature and Abbreviations

AOA	= angle of attack
b	= wing span
C_D	= drag coefficient
C_L	= lift coefficient
C_l	= rolling moment coefficient
C_m	= pitching moment coefficient
C_n	= yawing moment coefficient
CG	= center of gravity
Isp	= specific impulse
M	= flight or flow Mach number
MAC	= mean aerodynamic chord
p	= angular rate of rolling motion
V	= flight airspeed
α	= angle of attack
β	= side slip angle
δ	= deflection angle of elevator
δ_a	= deflection angle of aileron
δ_r	= deflection angle of rudder
ψ	= yaw angle

1 Introduction

Innovation in technologies for high-speed atmospheric flights is essential for establishment of supersonic/hypersonic and reusable space transportations. It is quite effective to verify such technologies through small-scale flight tests in practical high-speed environments, prior to installation to large-scale vehicles. Thus we are developing a small-scale supersonic flight experiment vehicle as a flying test bed.

We propose several candidate vehicle configurations and characterize their aerodynamics through wind tunnel tests. On the basis of their results, a twin engine configuration with a cranked-arrow main wing is selected as the baseline. Its aerodynamic stability and controllability are analyzed in detail through wind tunnel tests. These treatments and results will be elaborated in Section 2. On the other hand, a counter-rotating axial fan turbojet (CRAFT) engine is proposed for propulsion for this vehicle. Its concept and design will be outlined briefly in Section 3. On the basis of the aerodynamic characterization and propulsion design analysis, flight capability prediction is carried out by point mass analysis of motion. It will be described in Section 4. Prior to the construction of the supersonic vehicle, a prototype is designed and fabricated in order to verify the subsonic flying characteristics of the vehicle configuration through flight tests. Section 5 will outline the design of the prototype vehicle and its maiden flight test carried out in August 2010. A revised aerodynamic configuration with an air-turbo ramjet gas-generator cycle (ATR-GG) engine will be proposed and its aerodynamics will be assessed in Section 6. Then Section 7 will be conclusions.

2 Configuration Designs and Aerodynamic Characterization

2.1 Proposed Configuration Designs

Five configurations shown in Fig. 1 were proposed*. Their concepts are as follows:

- *M2005*: A single engine is installed in the fuselage and an intake is located at the nose, in order to minimize the projected front area and to place the thrust vector nearest to the fuselage axis. These would minimize parasite and trim drags.
- *M2006*: Twin engines are installed underneath the main wing at the both sides of the fuselage in order to attain sufficient acceleration and ascent capability. A diamond wing section of 6% thickness is adopted for reduction of

wave drag during supersonic flights. Its main wing has a cranked arrow planform for stable aerodynamic characteristics. A high wing configuration with a dihedral of 1.0 degree is also adopted in order to attain sufficient roll stability.

- *K2005*: A single engine is installed at the root of the vertical tail on the rear part of the fuselage. The main wing has a variable planform with sweep-back angles of 30 and 50 degrees. A canard is adopted instead of a horizontal tail.
- *K2006*: A slight extent of blended-wing-and-body feature is added to *K2005*; the connecting portions between the wings, the fuselage, and the engine nacelle are smoothed. This would reduce wing-body interference drag.
- *O2006*: A single engine is installed in the fuselage and two intakes are located on the both sides of the fuselage. A so-called close-coupled canard is equipped for enhancement of lift during subsonic flights.

On the basis of wind tunnel tests and engine performance prediction, the thrust margin, i.e. thrust minus parasite drag, was analyzed for various sets of flight Mach number and altitude. An optimistic assessment of attainability of supersonic flight was carried out using the thrust margin map where the aspect of fuel consumption was neglected. As a result of this analysis, the twin engine configuration *M2006* was found to be the only one capable of attaining supersonic flights. Thus *M2006* was selected as the baseline configuration. Its overall shape and dimensions are illustrated in Fig. 2. It has ailerons, a rudder, and all-pivoting horizontal tails as control surfaces.

In addition, a modified configuration *M2006prototype* was proposed for construction of a prototype vehicle, in which the following modifications were adopted as shown in Fig. 3:

- (a) Its horizontal and vertical tails are enlarged and less swept back for enhancement of stability and controllability during takeoff and landing.
- (b) Its lateral control capability is enhanced by adopting all-pivoting elevons.

*Their codenames consist of a prefix M, K, or O and four digits. The prefix is for the name of the institution, i.e. Muroran Institute of Technology, Kyusyu University, or Osaka Prefecture University, by whom the configuration was proposed. The four digits are for the fiscal year of the proposition.

DEVELOPMENT OF A SMALL-SCALE SUPERSONIC FLIGHT EXPERIMENT VEHICLE AS A FLYING TEST BED

- (c) A pair of inboard flaps is installed for takeoff and landing.
- (d) Its engine nacelles are connected to the fuselage on its both sides for the sake of convenience in fabrication and maintenance.
- (e) Its nose is extended forward in order to attain a sufficient capacity for installing fuel and avionics in the fuselage.

Series of wind tunnel tests were carried out for these configurations M2006 and M2006prototype. The results will be outlined in the following subsections.



(a) M2005



(b) M2006



(c) K2005



(d) K2006



(e) O2006

Fig. 1. Proposed aerodynamic configurations.

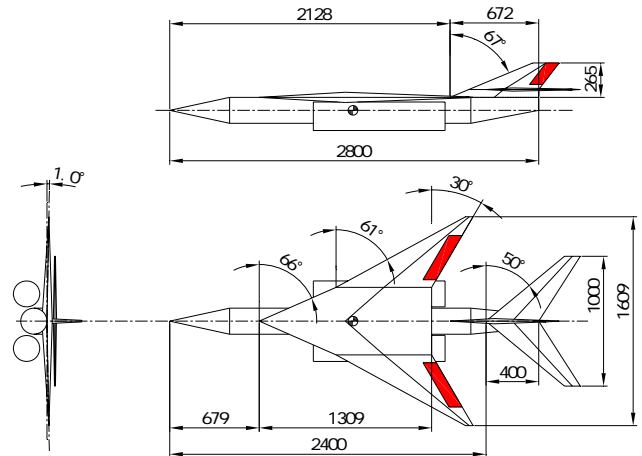


Fig. 2. The baseline configuration M2006. It has all-pivoting horizontal tails.

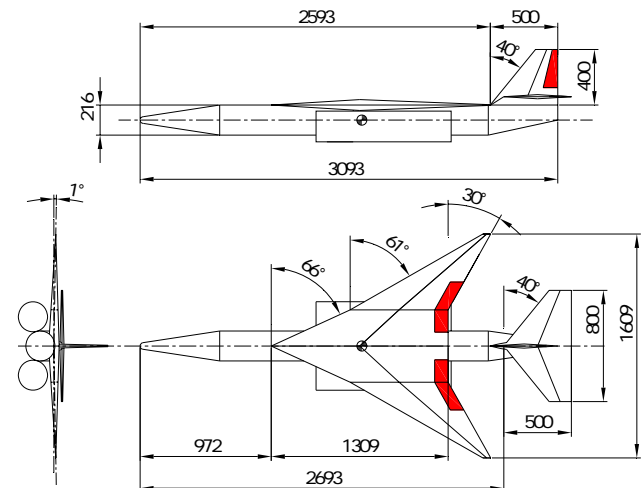


Fig. 3. The modified configuration M2006prototype for constructing a prototype vehicle.

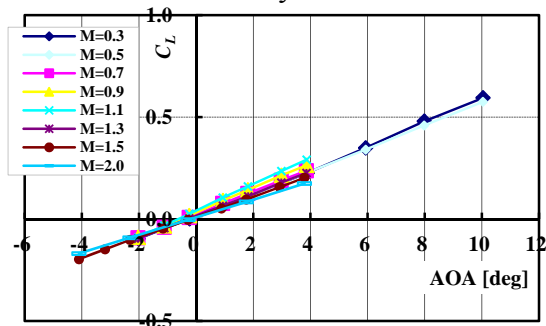
2.2 Lift and Drag Characteristics

The Comprehensive High-speed Flow Test Facility at the Institute of Space and Astronautical Science (ISAS) of the Japan Aerospace Exploration Agency (JAXA) was used for the present aerodynamic characterization. The facility consists of a transonic wind tunnel for Mach 0.3 to 1.3 and a supersonic wind tunnel for Mach 1.5 to 4.0. The

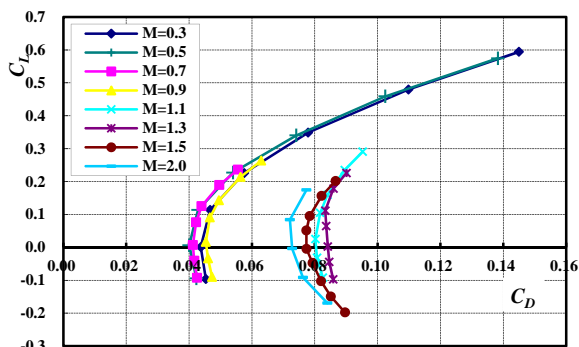
cross-sectional size of their test sections are 600x600mm.

The results for lift and drag are shown in Fig. 4. The maximum value of the angle of attack (AOA) is 10 degrees for subsonic conditions and 4 degrees for transonic/supersonic conditions. These small values are correspondent to the force capacity of the internal balance utilized. The lift coefficient curves show quite a good linearity with a slope of 0.058/deg for subsonic, 0.065/deg for transonic, and 0.043/deg for supersonic regime, where the elevators are fixed. The so-called sound barrier, i.e. the drag peak at transonic regime, is small owing to the large sweep-back angles of the wing and tails.

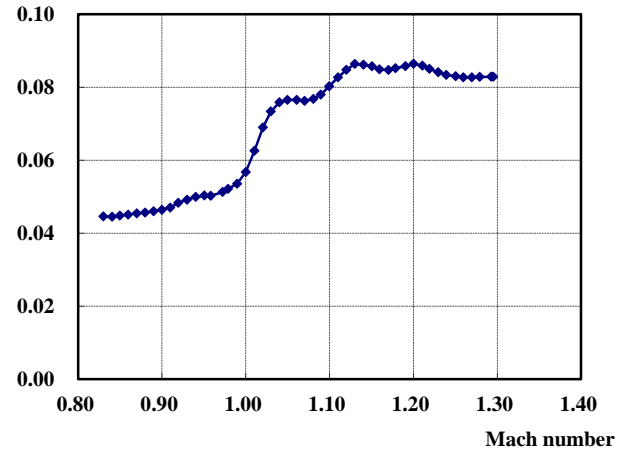
Concerning the configuration M2006prototype, additional subsonic wind-tunnel tests were carried out at Osaka Prefecture University. Their results are shown in Fig. 5 for AOA ranging from -30 to +30degrees. The linearity of its lift coefficient is found to be good for this wide range of positive AOA, owing to the stability of the vortex system over the present cranked-arrow wing with a large inboard sweepback angle of 66deg[1]. The linearity deteriorates for negative AOA probably because the engine nacelles would interfere with the vortex system.



(a) Lift coefficient versus angle of attack.



(b) Drag polar.



(c) Mach number dependence of the drag coefficient at a zero angle of attack.

Fig. 4. Lift and drag characteristics of the baseline configuration M2006.

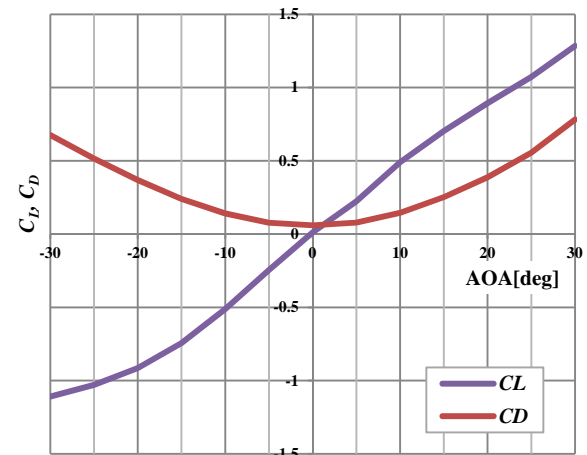


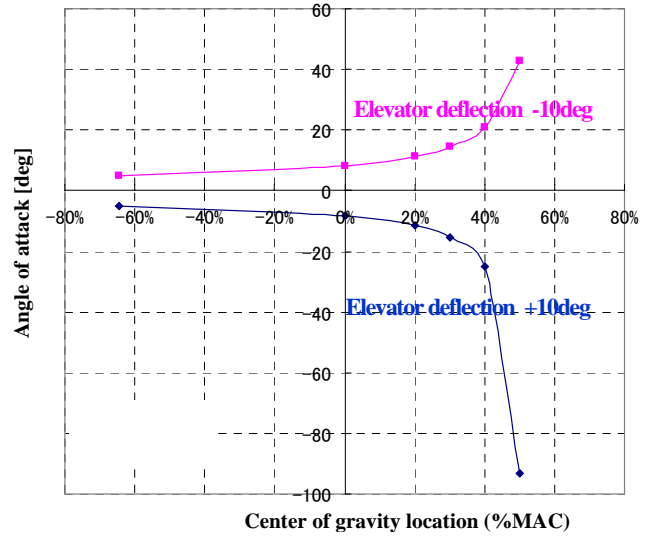
Fig. 5. Subsonic lift and drag characteristics of the modified configuration M2006prototype.

2.3 Trim Capability for Pitching Motion

The measured variation of the pitching moment coefficient C_m with varying AOA is shown in Fig. 6 (a) and (b) for a centre of gravity (CG) location of 20% of the mean aerodynamic chord (MAC) and for several elevator deflection angles ranging from -10 to +10 degrees. Note that the elevator deflection measures positive when the trailing edge of the elevator deflects downwards. The negative gradients of the curves indicate static stability in the pitching motion. The value of the gradient, i.e. the extent of the stability, varies in accordance with the CG location; the more forward the CG lies, the larger the stability is. On the other hand, the intercepts on the horizontal AOA axis represent the trim conditions. For example, at Mach 0.3

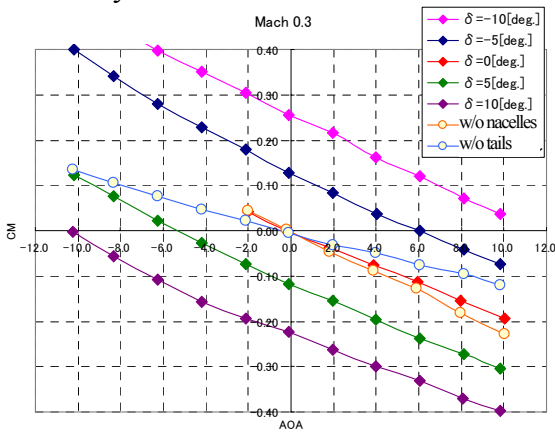
the vehicle can attain pitch trim at AOA of 6.0 degrees with an elevator deflection of -5 degrees for a CG location of 20%MAC.

Fig. 6 (c) shows the pitch trim capability for various CG locations, where the upper magenta curve indicates the AOA for pitch trim at each CG location for an elevator deflection of -10 degrees, and the lower blue curve for an elevator deflection of +10 degrees. So the difference in AOA between the two curves is the range where pitch trim can be attained. The more forward the CG is located, the narrower the AOA range for pitch trim is, and vice versa. Note that the more backward CG location than 40%MAC will cause pitching instability. A CG location of 25 to 30%MAC is found to be appropriate for both the pitch trim capability and stability.

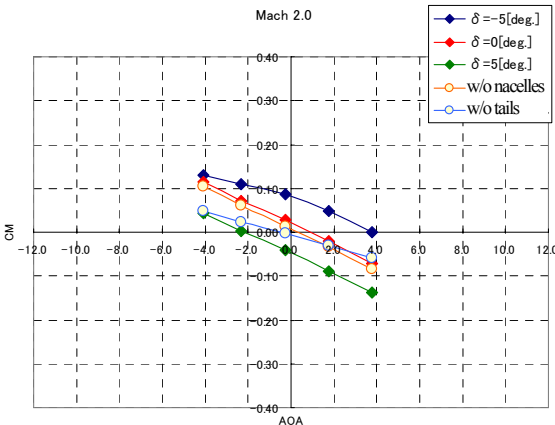


(c) Pitch trim capability at Mach 0.3.

Fig. 6. Pitching moment characteristics measured by wind tunnel tests.



(a) Pitching moment coefficient versus angle of attack for several elevator deflections with a CG location of 20%MAC and at Mach 0.3.



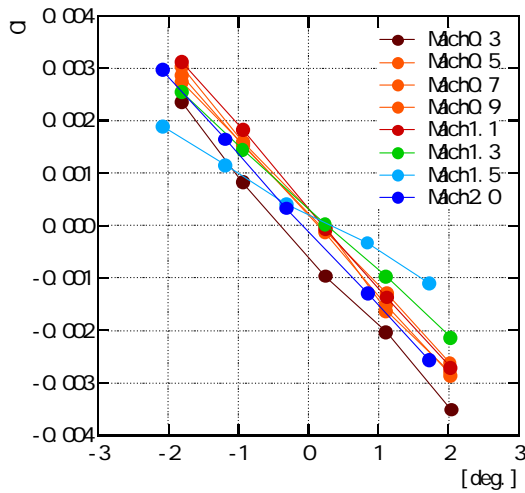
(b) Pitching moment coefficient versus angle of attack for several elevator deflections with a CG location of 20%MAC and at Mach 2.0.

2.4 Trim and Control Capability for Rolling Motion

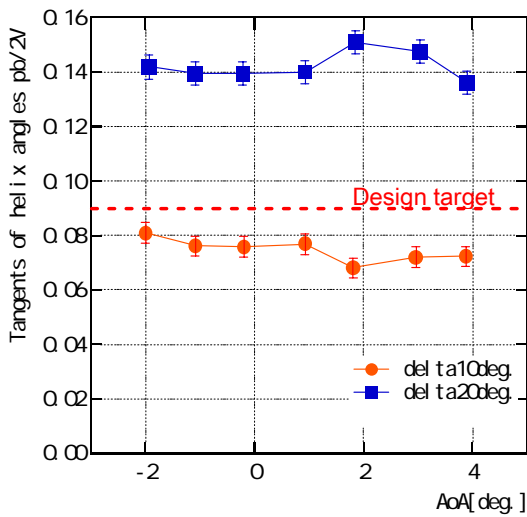
Fig. 7 (a) shows the measured rolling moment coefficient C_l versus the side slip angle β for several Mach numbers. The static roll stability is indicated by the negative gradients of the curves for all of the Mach numbers. For assessment of the roll control capability, the tangent of helix angle $pb/2V$ is a convenient measure, where p is the angular rate of the rolling motion, b is the wing span, and V is the airspeed. This helix angle means the angle at which the main wing tips draw a pair of helices during a rolling maneuver. It depends theoretically only on aircraft's geometry and is independent of dimension, airspeed and angle of attack. It can be estimated from wind tunnel test data using the following equation [2]:

$$\frac{pb}{2V} = \frac{C_{l,\delta_a} \delta_a K}{2C_{l,p}} \quad (1)$$

where the roll damping derivative $C_{l,p}$ and the correction factor for large aileron deflections K are empirical factors [2]. Its values evaluated from the present wind tunnel tests are shown in Fig. 7 (b) for aileron deflections of 10 and 20 degrees. The dotted red line indicates a design target for acrobatic/fighter aircraft. Thus sufficient roll control capability is predicted for the present M2006 configuration.



(a) Rolling moment coefficient versus side slip angle for several Mach numbers ranging from 0.3 to 2.0.



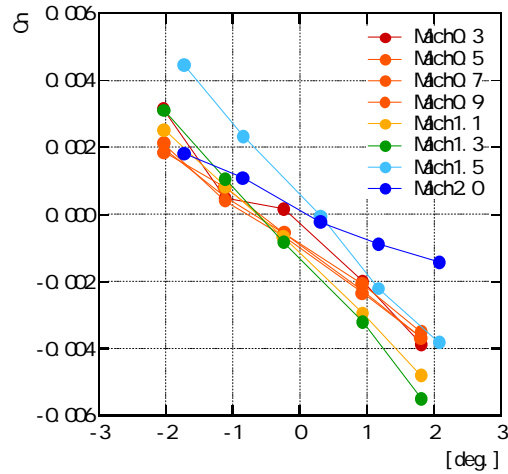
(b) Estimated tangent of helix angle main wing tips draw at Mach 0.7.

Fig. 7. Rolling moment characteristics measured by wind tunnel tests.

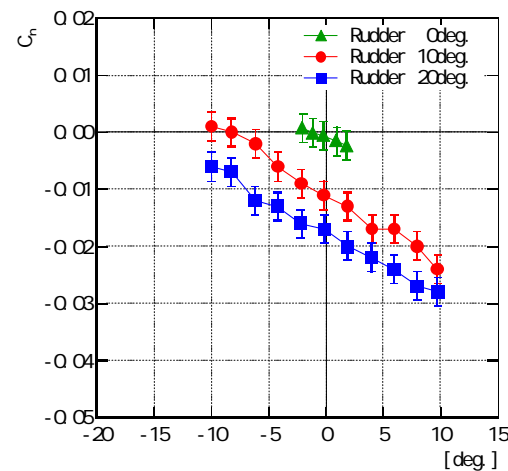
2.5 Trim and Control Capability for Yawing Motion

Fig. 8 (a) shows the measured yawing moment coefficient C_n versus the yaw angle ψ for several Mach numbers. The static yaw stability is indicated by the negative gradients of the curves for all of the Mach numbers. Fig. 8 (b) shows the yaw trim capability. The intercepts on the horizontal axis represent the trim conditions. Thus yaw trim can be attained at yaw angles of -8 or -16 degrees with rudder deflections of 10 or 20 degrees, respectively. The rudder power $C_{n,\delta_r} \equiv \partial C_n / \partial \delta_r$ evaluated from the present wind tunnel tests is shown in Fig. 8 (c) where the

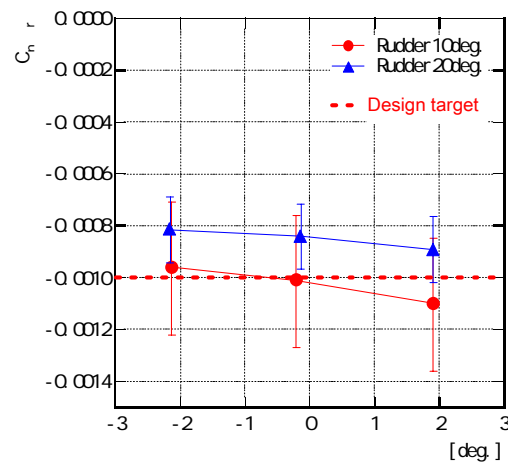
dotted red line is a design target. Thus sufficient rudder effectiveness is predicted for the present M2006 configuration.



(a) Yawing moment coefficient versus yaw angle for several Mach numbers ranging from 0.3 to 2.0.



(b) Yawing moment coefficient versus yaw angle for some rudder deflections at Mach 0.7.



(c) Rudder power for some rudder deflections.

Fig. 8. Yawing moment characteristics measured by wind tunnel tests.

3 Concept and Design of the Proposed Engine

A counter-rotating axial fan turbojet (CRAFT) engine was proposed and designed preliminarily for installation onto the proposed supersonic flight experiment vehicle [3-5]. In this engine the rotor fans in the first and the second stages rotate in an opposite direction and the stator fans can be eliminated to establish a compactness of the engine configuration. Its thrust and specific impulse evaluated for an afterburner fuel/air ratio of 0.025 by a thermodynamic cycle analysis are shown in Fig. 9. The operational upper boundary in terms of flight Mach number is correspondent to the constraint on the turbine inlet temperature (TIT). For more practical design of the engine components, CFD analysis has been carried out using the turbo-machinery analysis software FineTURBO as illustrated in Fig. 10. A set of prototype counter-rotating fans was fabricated and is undergoing ground rig tests.

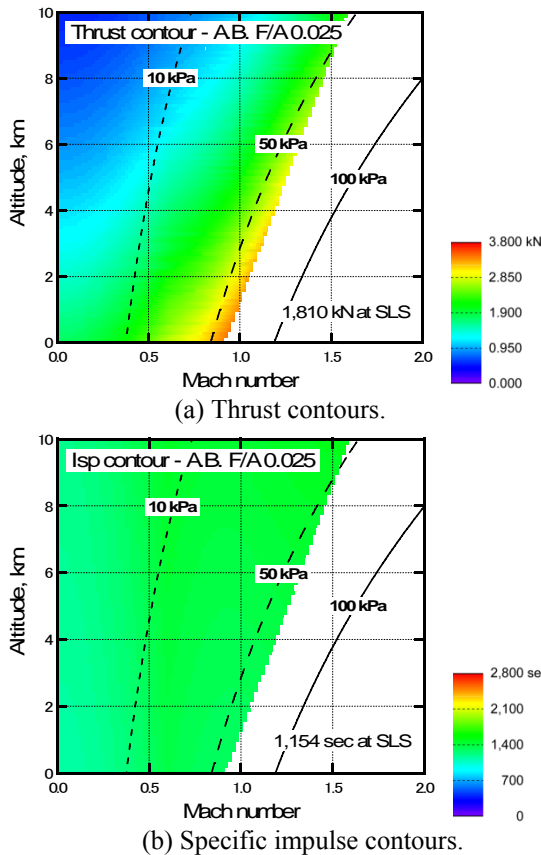


Fig. 9. Predicted performance of the proposed counter-rotating axial fan turbojet engine at an afterburner fuel/air ratio of 0.025.

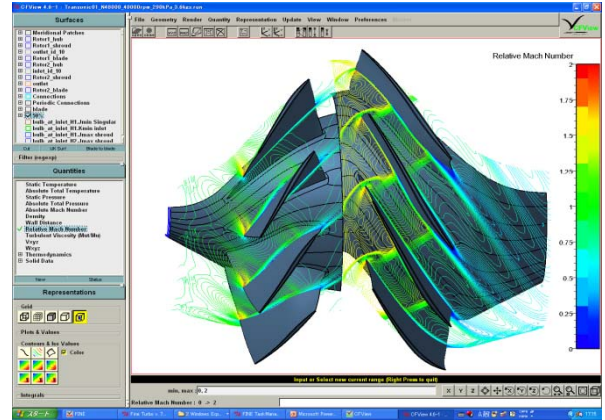


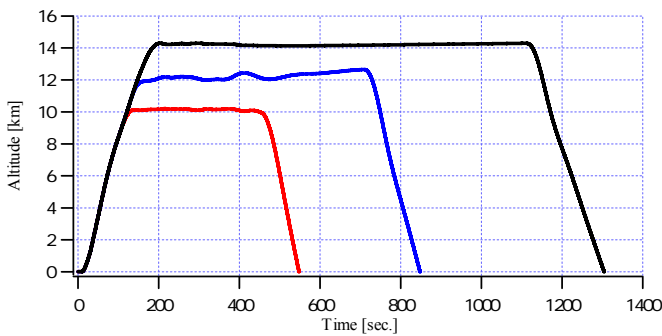
Fig. 10. CFD analysis of counter-rotating axial fans for the proposed turbojet engine.



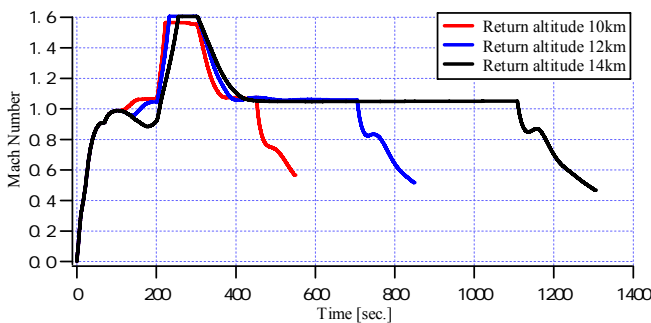
Fig. 11. The fabricated first-stage fan in the prototype counter-rotating axial fan turbojet engine.

4 Flight Capability Prediction

Flight capability of the proposed supersonic experiment vehicle is predicted by point mass analysis on the basis of the lift and drag characteristics measured by wind tunnel tests, thrust and specific impulse evaluations of the proposed engine, and a preliminary weight estimation of the airframe. One of the results is shown in Fig. 12, where three flight trajectories with return cruise at altitudes of 10, 12, and 14 km are illustrated. It is found that the vehicle can attain supersonic flight at Mach 1.6 for about one minute and a sufficient endurance for return flight. The upper limit in flight Mach number is correspondent to that in the turbine inlet temperature of the proposed engine design. This constraint can be eliminated in the proposed revision engine, i.e. an air-turbo ramjet gas-generator cycle (ATR-GG) engine.



(a) The history of altitude.



(b) The history of Mach number.

Fig. 12. One of the results of the flight capability analysis.

5 A Prototype Vehicle for Subsonic Flight Tests

5.1 Configuration Design and Fabrication

Prior to construction of the supersonic vehicle, a prototype with the modified configuration M2006 prototype was designed and fabricated in order to verify the subsonic flying characteristics of the vehicle configuration through flight tests. Its overall appearance is shown in Fig. 13.

It has semi-monocoque structure composed of spars, stringers, and skins made of CFRP and ribs and ring frames made of wood. The forward part of fuselage is made of GFRP so as to install antennas inside. The empty mass is 22.2kg including a propulsion system. The maximum fuel mass is 4.6kg, and the avionics is 0.2kg. Then the total takeoff mass is 27.0kg. The propulsion system is model-scale twin turbojet engines available on the market. Their rated total thrust is 330N and the maximum airspeed for level flight is predicted to be 104m/sec according to the wind-tunnel tests. Its nickname

is OHWASHI (Steller's Sea Eagle) which was selected by an advertised prize contest.



(a) The airframe before painting.



(b) The painted and fully equipped vehicle.

Fig. 13. Overall appearance of the fabricated prototype vehicle.

5.2 First Flight Test

The first flight test of the prototype vehicle was carried out in August 2010 at the Shiraoi Airfield nearest to Muroran Institute of Technology. The length of the runway is 800m. The vehicle was radio-controlled by a pilot on the ground. For onboard data acquisition, a combined GPS/INS navigation recorder, an air-data-sensor (ADS) including a 5-hole Pitot tube, a control signal recorder, two electric control units for the twin turbojet engines, and a small video camera were installed onboard. A snapshot of the preflight check on the onboard avionics is shown in Fig. 14. The appearance of the prototype vehicle ascending just after takeoff is shown in Fig. 15. The vehicle circled six times above and around the runway for 4 minutes and a half. Its flight stability and controllability were quite adequate.

Its flight trajectory is illustrated in Fig. 16 on the basis of the onboard GPS data. The airspeed and angles of attack and sideslip estimated from the ADS data show twelve high-speed flights and twelve low-speed turns with pitch-up attitudes and sideslips, in accordance with the six rounds, as shown in Fig. 17. The maximum air speed 58m/sec is considerably smaller than prediction due to drag enhancement described below.

Because control inputs for the control surfaces and engine throttle were quite frequent in the flight test, local-quasi-steady data were extracted from the overall data acquired. Aerodynamic coefficients were estimated from the acceleration and angular rates so extracted and the thrust characteristics measured by ground tests. The results for lift and drag coefficients in quasi pitch-trim conditions are shown in Fig. 18 in comparison with wind-tunnel data. The lift coefficients from the flight test agree quite well with those from wind-tunnel tests. Note that the lift curve slope in the pitch-trim condition is smaller than that in fixed-elevator condition since a downward lift on the horizontal tail is required for pitch trim. On the other hand, parasite (i.e. zero-lift) drag is enhanced as shown in Fig. 18 (b) due to structural members installed between the engines and the nacelle internal walls.



Fig. 14. Preflight check on onboard avionics.



Fig. 15. The prototype vehicle ascending just after takeoff.

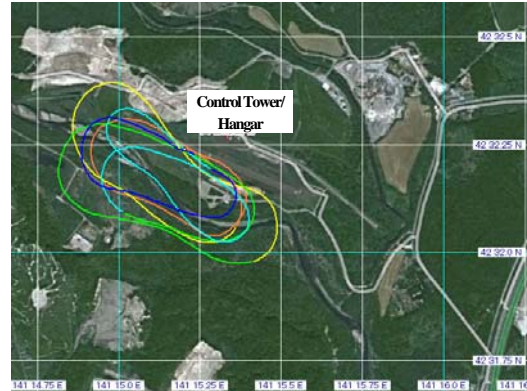


Fig. 16. The flight trajectory measured with onboard GPS receiver.

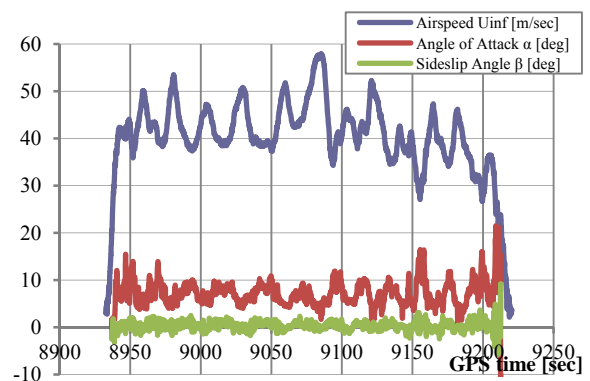
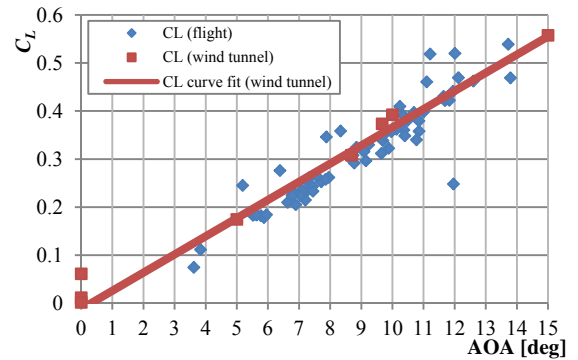
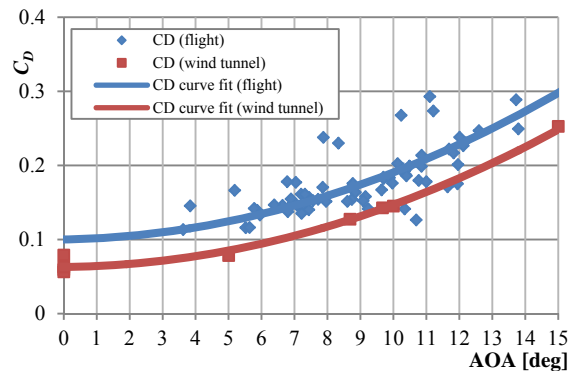


Fig. 17. ADS data acquired in the flight test.



(a) Lift coefficient versus angle of attack.



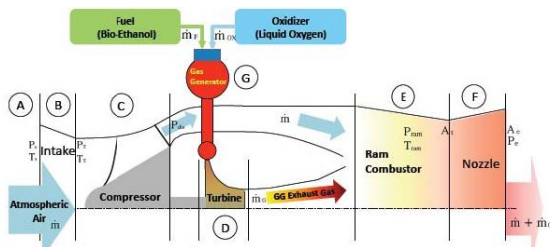
(b) Drag coefficient versus angle of attack.

Fig. 18. Aerodynamic coefficients estimated from the flight test in comparison with wind-tunnel test data rearranged for pitch-trim conditions.

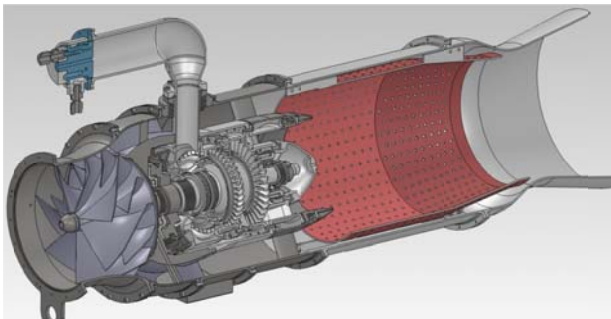
6 A Revised Configuration

6.1 A Revision Engine

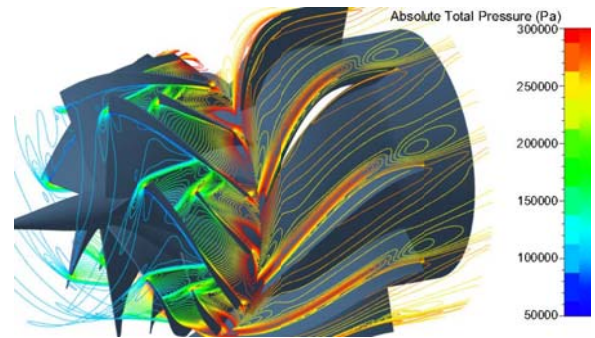
An air-turbo ramjet gas-generator cycle (ATR-GG) engine is being designed for improvement in thrust at supersonic flights[6]. Its conceptual schematic is shown in Fig. 19 (a). Its turbine inlet condition is independent of the flight condition since the turbine is driven by the gas generator. Thus this type of engine is quite suitable to supersonic flights. The thrust and Isp of the proposed engine are rated at 3.8kN and 570sec respectively at SLS condition, and 2.3kN and 720sec respectively at an altitude of 17km and Mach 2.0 (dynamic pressure 25kPa). The 3-D view of the proposed design is illustrated in Fig. 19 (b). Compressor fans and turbine blisks were designed using the turbomachinery design software AxCent and their fluid-dynamics were analyzed using the turbomachinery analysis software FineTURBO as shown in Fig. 19 (c). The turbine blisks, turbine nozzles and guide vanes of a prototype engine have been fabricated. They are to be applied to ground rig tests in this fiscal year.



(a) A conceptual schematic.



(b) 3-D view of the engine design.



(c) CFD analysis of the compressor fans.
Fig. 19. The proposed ATR-GG engine.

6.2 A Revised Aerodynamic Configuration

A revised aerodynamic configuration M2011 with a single ATR-GG engine is designed as shown in Fig. 20. Its wing and tail geometries are rigorously similar to that in the prototype vehicle; most of the aerodynamic data for the configurations M2006 and M2006prototype can be applied to the M2011. Its wingspan and fuselage diameter are enlarged by a factor of 1.5 so as to install an ATR-GG engine with a diameter of 230mm and to retain the ratio of wingspan to fuselage diameter. Three types of fuselage length, 5.8m, 6.8m, and 7.8m, are considered for various quantity of fuel installed. In addition, three types of air-intake length are considered so as to allow uncertainty in intake design.

The longitudinal aerodynamics of the M2011 were measured by wind-tunnel tests as shown in Fig. 21. Its lift and drag characteristics are quite similar to those for the M2006 and M2006prototype. Its pitching moment characteristics are adequate for all Mach numbers ranging from 0.3 to 2.0. In addition, the influence of the large nose lengths on the longitudinal aerodynamics is found to be small.

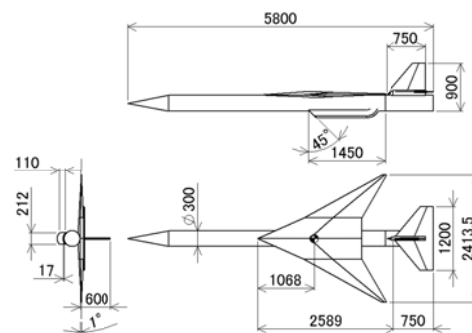
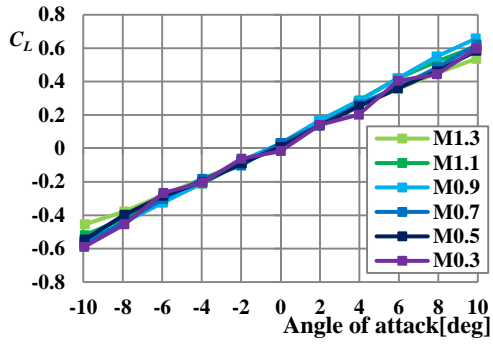
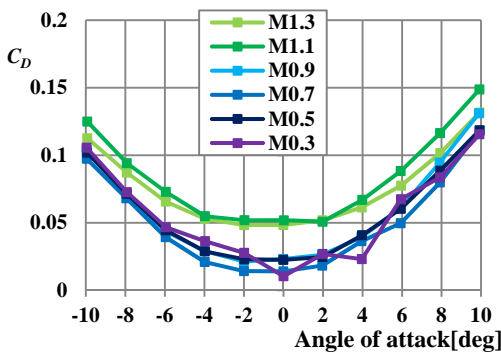


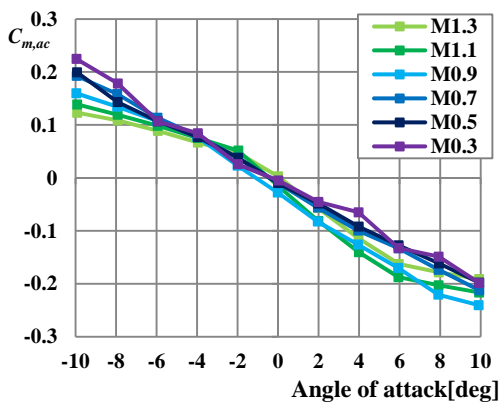
Fig. 20. The proposed revision configuration M2011.



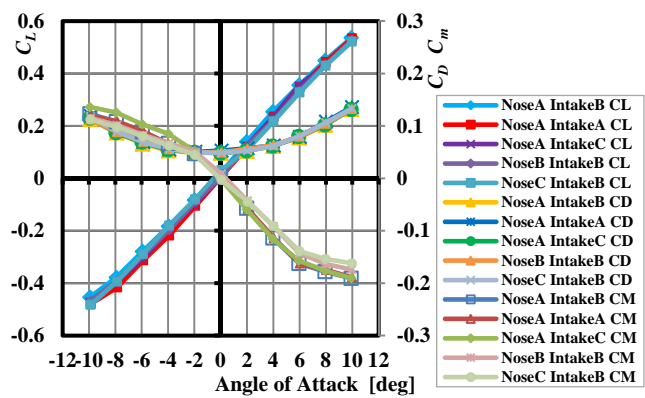
(a) Lift coefficient.



(b) Drag coefficient.



(c) Pitching moment coefficient around the aerodynamic center of the main wing.



(d) Lift, drag, and pitching moment coefficients for several sets of nose and intake lengths.

Fig. 21. Longitudinal aerodynamics measured by wind tunnel tests for the configuration M2011.

6.3 Flight Capability Prediction

Flight trajectory analysis of the vehicle with an ATR-GG engine and the M2011 aerodynamics was carried out. Its results shown in Fig. 22 predict that a drag reduction of 15% will enable achievement of flight Mach number 2.0. Such drag reduction could be attained by adopting the so-called area rule to the aerodynamic configuration of the vehicle.

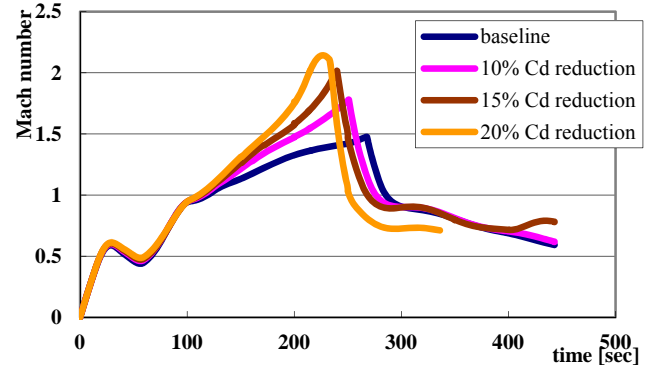


Fig. 22. Results of the flight capability analysis of the M2011 vehicle with the proposed ATR-GG engine. Ten to twenty percent of drag reduction is assumed.

7 Conclusions

With the aims of creating and validating innovative fundamental technologies for high-speed atmospheric flights, a small scale supersonic experiment vehicle was designed as a flying test bed. Several aerodynamic configurations were proposed and analyzed by wind tunnel tests. A twin-engine configuration was selected as the baseline. Its flight capability was predicted by point mass analysis on the basis of aerodynamic characterization and propulsion performance estimation. In addition, a prototype vehicle with the almost equivalent configuration and dimension was designed and fabricated for verification of subsonic flight characteristics. Its first flight test was carried out in August 2010 and good flight capability was demonstrated.

Furthermore a revised aerodynamic configuration and an air-turbo ramjet gas-generator cycle (ATR-GG) engine are being designed for improvement in flight capability at higher Mach numbers.

An autonomous guidance and control system will be designed on the basis of the acquired

aerodynamics data. In addition, structure of the airframe will be revised, and the design of the proposed ATR-GG engine will be improved to fabricate actual engines for supersonic flights.

Then the proposed supersonic flight experiment vehicle will be realized in near future. This prospective flight experiment vehicle will be applied to flight verification of innovative fundamental technologies for high-speed atmospheric flights such as turbo-ramjet propulsion with endothermic or biomass fuels, MEMS and morphing techniques for aerodynamic control, aero-servo-elastic technologies for efficient aerodynamic control with low-stiffness structure, etc.

Acknowledgements

The authors would like to express cordial gratitude to JAXA/ISAS for having given opportunities of wind tunnel tests at its Comprehensive High-speed Flow Test Facility as well as to Associate Professor Takeshi Tsuchiya, Dr. Masaru Naruoka, and Mr. Takuma Hino of University of Tokyo for their arrangement of the GPS/INS navigation avionics and the ADS circuit. The authors also express thanks to Professor Takakage Arai of Osaka Prefecture University and Professor Shigeru Aso and Associate Professor Yasuhiro Tani of Kyusyu University for their propositions on vehicle configuration design.

References

- [1] Kwak D, Rinoie K and Kato H. Longitudinal Aerodynamics at High Alpha on Several Planforms of Cranked Arrow Wing Configuration, *2010 Asia-Pacific International Symposium on Aerospace Technology*, Xian, China, September 13-15, 2010.
- [2] Perkins CD and Hage RE. *Airplane Performance Stability and Control*, John Wiley & Sons, 1949.
- [3] Minato R, Ota T, Fukutomi K, Tanatsugu N, Mizobata K, Kojima T, Kobayashi H. Development of Counter Rotating Axial Fan Turbojet Engine for Supersonic Unmanned Plane, *Joint Propulsion Conference 2007*, AIAA Paper 2007-5023, Cincinnati, USA.
- [4] Minato R, Himeno T, Kojima T, Kobayashi H, Taguchi H, Sato T, Arai T, Mizobata K, Sugiyama H, Tanatsugu N. Development of Counter Rotating

Axial Fan Turbojet Engine for Supersonic Unmanned Plane at Muroran Institute of Technology, *International Gas Turbine Congress*, Tokyo, 2007.

- [5] Minato R, Kato D, Higashino K, Tanatsugu N. Development Study on Counter Rotating Fan Jet Engine for Supersonic Flight, ISABE 2011-1233, Goteburg, Sweden, 2011.
- [6] Minato R, Higashino K, Tanatsugu N. Design and Performance Analysis of Bio-Ethanol Fueled GG-cycle Air Turbo Ramjet Engine, *AIAA Aerospace Science Meeting 2012*, Nashville, Tennessee, USA, 2012.

Copyright Statement

The authors confirm that they, and/or their company or organization, hold copyright on all of the original material included in this paper. The authors also confirm that they have obtained permission, from the copyright holder of any third party material included in this paper, to publish it as part of their paper. The authors confirm that they give permission, or have obtained permission from the copyright holder of this paper, for the publication and distribution of this paper as part of the ICAS2012 proceedings or as individual off-prints from the proceedings.